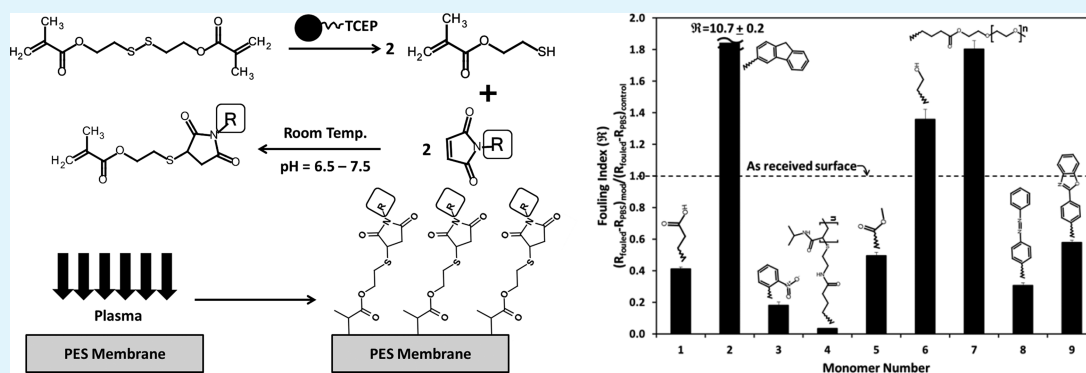


A New Combinatorial Method for Synthesizing, Screening, and Discovering Antifouling Surface Chemistries

Joseph Imbrogno, Matthew D. Williams, and Georges Belfort*

Howard P. Isermann Department of Chemical and Biological Engineering and The Center for Biotechnology and Interdisciplinary Studies, Rensselaer Polytechnic Institute, Troy, New York 12180, United States

Supporting Information



ABSTRACT: A set of diverse monomers were synthesized using combinatorial chemistry and tested using our unique high-throughput screening platform. The versatility of our platform is exemplified by possible applications in reducing biological fouling on ship hulls, filtration membranes, and surgical instruments, to name a few. To demonstrate its efficacy, the novel monomers were graft-polymerized onto light sensitive poly(ether sulfone) (PES) membranes via atmospheric-pressure plasma polymerization. A diverse library was synthesized by reacting a common vinyl ester linker with a library of maleimides containing various different functional groups. This allowed us to produce a library of many different surfaces and graft them all using the same linker chemistry. The modified surfaces were then tested and screened for the best antiprotein adsorption (nonfouling) properties. Membranes, functionalized with carboxylic acid, zwitterionic, and ester groups, had the lowest protein adhesion compared with that of an unmodified control PES membrane after a static fouling test. After dynamic fouling, these same functionalities as well as a hydroxyl group exhibited the highest permeability. These monomers performed better than our best previously synthesized amide monomers as well as our best poly(ethylene glycol) monomers, which are known to have very high protein resistance. Hansen solubility parameters qualitatively predicted which monomers performed best, indicating favorable interactions with water molecules.

KEYWORDS: combinatorial chemistry, antiprotein fouling surfaces, high-throughput screening, atmospheric-pressure plasma

1. INTRODUCTION

Biological fouling is a major limitation in many applications, including marine structures such as ship hulls and oil rigs,¹⁻⁶ surgical instruments,⁷ food and biotechnology processing,⁸⁻¹⁰ and wastewater treatment.¹¹⁻¹³ A facile, fast, and inexpensive method for assisting in the discovery of new low fouling coatings for these applications is urgently needed.^{14,15} To meet this need, we present a novel combinatorial chemistry method combined with our unique high-throughput platform for synthesizing, screening, testing, and discovering low fouling chemistries. Some of the chemistries discovered here are novel [tricyclic (2), ester (5), azo (8), and heterocyclic (9) R groups], while others [amide (4), carboxylic acid (1), zwitterionic (3), poly(ethylene glycol) (PEG) (7), and hydroxyl (6) R groups] have been known for some time.^{16,17} To demonstrate the efficacy of the method and the discovery of

new low fouling surface chemistries, we chose membrane ultrafiltration of protein solutions as an example.

Combinatorial chemistry has become very attractive in recent years.^{18,19} This method uses a modular approach to synthesize new molecules by combining carbon heteroatoms and "spring-loaded reactants".²⁰ The ability to combine many different types of chemistry is extremely useful for high-throughput screening techniques,²¹ when reaction mechanisms are poorly understood, such as in organometallics,²² and when developing new catalysts,²³ to name a few. This method reduces the required amount of synthesis time by limiting the number of reaction steps.

Received: October 10, 2014

Accepted: January 8, 2015

Published: January 8, 2015

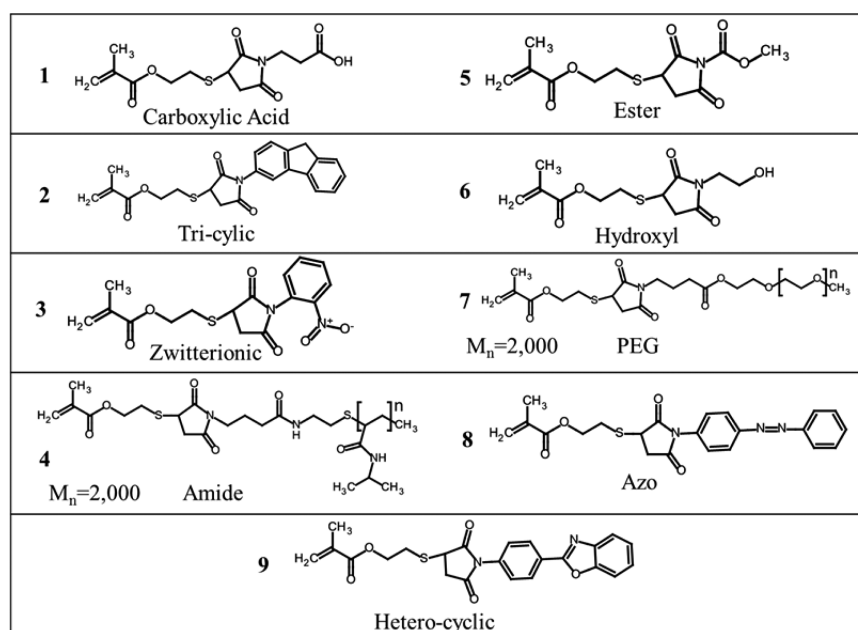


Figure 1. Structures of all nine synthesized monomers. Monomers were synthesized by reacting the thiol linker with a maleimide containing various different functional groups (attached to the nitrogen in the maleimide ring).

Ultrafiltration membranes are widely used in the biotechnology, food, beverage, and water industries. The major limitations of using membrane filtration in these industries are fouling (adhesion of interacting retained solutes like proteins, viruses, DNA, and cells) and concentration polarization (buildup of noninteracting retained solutes like ions near the membrane surface), which ultimately lead to a decrease in performance and an increase in energy use. A major source of fouling is the binding of nonspecific protein to the membrane surface.^{24,25} As upstream feed titers increase, especially in the biotechnology industry, the majority of the operating costs of the entire process are shifted heavily to the downstream processes.^{26,27} Thus, new high-performance low fouling synthetic membranes are needed. High-throughput surface chemistry modification of membranes is an effective and economic method for screening, identifying, and developing membranes with new surface chemistries.

Previous work has indicated that water interactions at surfaces likely play a critical role in interactions of protein with membranes.^{21,28–30} Special focus will be given to the role of water interactions to gain a fundamental understanding of membrane fouling from proteins. The Hansen solubility parameter calculations (δ_d , δ_p , and δ_h) predict that hydrophilic monomers, which have solubility parameters close to those of water, should perform the best.²¹

In this work, we utilize a unique high-throughput (HTP) platform with an atmospheric-pressure plasma (APP) polymerization system to modify irradiation sensitive commercial poly(ether sulfone) (PES) membranes. APP is commercially attractive because it operates at atmospheric pressure and can be easily incorporated into membrane production lines, is flexible (both graft monomer and membrane material can be varied), and is economical (vacuum not required for graft polymerization). A vast number of new surface chemistries (library) can be produced using combinatorial methods to expand the breadth of our monomer library. The effect of carbon chain length on antifouling properties has recently been reported.²¹ That study showed that a certain minimal chain

length is required (four to six carbons) for hydroxyl and PEG monomers to be antifouling. If the chain length is too short or too long, either a negligible decrease or an increase in fouling will occur, respectively. Additionally, the spacing between nitrogen atoms in an amine/amide monomer appears to have an influence, as well.

In this work, the effect of new functional graft-polymerized groups on filtration performance was tested. Nine new monomers were synthesized, including carboxylic acid, zwitterionic, mixed matrix, azo, and heterocyclic classes. Some of these monomers, like PEG and zwitterionic, are expected to perform well on the basis of previous research.^{16,17,31–35} The newly synthesized monomers were then grafted and polymerized without purification on the surface of multiple light sensitive PES membranes located at the base of filter wells in 96-well plates. Permeation flux and solute transport across the modified membranes were measured spectroscopically before and after exposure to a static and dynamic fouling challenge. Using this high-throughput screening process, nine different surface chemistries were compared in a single afternoon with high reproducibility and confidence. The selected winners were determined by measuring a series of relevant parameters such as fouling index, solute selectivity, resistance (inversely proportional to flux), and theoretically estimated Hansen solubility parameters. From our new monomer sets, the monomers—carboxylic acid, zwitterionic, and ester-terminated—were closest to the bulk water solubility parameter value and exhibited the best performance. Thus, using the Hansen solubility parameters, the nearer and farther the loci for the grafted monomers with respect to the water locus, the lower and higher the fouling index, respectively. This qualitatively supports the idea that hydrophilic monomers perform the best and provides an *a priori* estimate of how new monomers will perform as protein resistant surfaces.

2. EXPERIMENTAL SECTION

2.1. Materials. Bis(2-methacryloyl)oxyethyl disulfide (99%), *N*-maleoyl- β -alanine (97%), 2-maleimidofluorene (99%), *N*-(2-

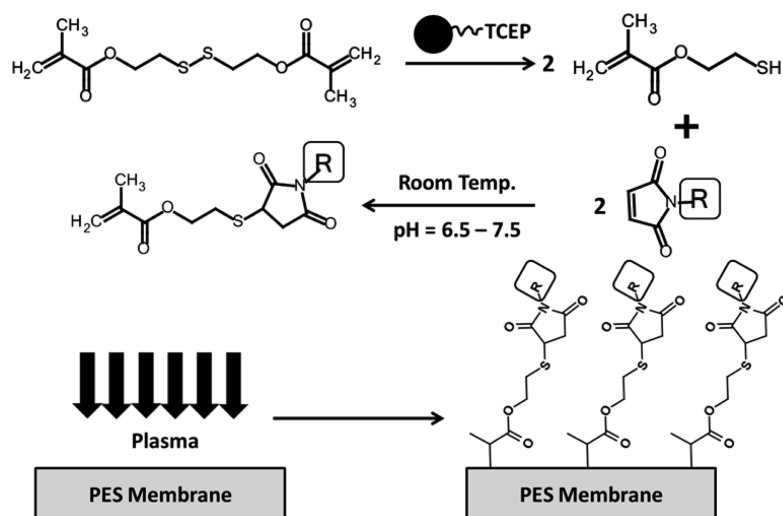


Figure 2. Reaction scheme for the combinatorial chemistry approach. A diverse library was generated by varying the R group in the square box. After synthesis, the monomers were grafted to 100 kDa MWCO poly(ether sulfone) ultrafiltration membranes at the bottom of 96-well filter plates using APP polymerization.

nitrophenyl)maleimide (99%), 4-phenylazomaleinanyl (97%), *N*-(2-hydroxyethyl)maleimide (97%), *N*-[4-(2-benzoxazolyl)phenyl]-maleimide (99%), *N*-methoxycarbonylmaleimide (>97%), poly-(ethylene glycol) methyl ether maleimide (99%; $M_n = 2000$), and poly(*N*-isopropylacrylamide), maleimide terminated (99%; $M_n = 2000$) were purchased from Sigma-Aldrich (St. Louis, MO) and used without further purification. An immobilized TCEP disulfide reducing gel was purchased from Thermo Scientific (Rockford, IL). Spin filter tubes and receiving tubes (2 mL) were obtained from Novagen (Darmstadt, Germany); 96-well filter plates (CMR# 1746-3, Seahorse Labware, Chicopee, MA) were used for HTP grafting and filtration. PES membranes (100 kDa MWCO) with an effective area of 19.95 mm² were mounted and heat-sealed by the manufacturer (Seahorse Bioscience, North Billerica, MA) in the bottom of each well of a 96-well filter plate (each well has a volume of 400 μ L). The membranes were washed and soaked in deionized (DI) water overnight before use to remove surfactant. Industrial grade helium and oxygen gases were used as a plasma source (Airgas, Albany, NY). The solution for the static protein fouling assay was prepared by dissolving 1 mg/mL bovine serum albumin (BSA) [>96%, molecular weight (MW) of \sim 67 kDa, pI 4.7] in a phosphate-buffered saline (PBS) solution. BSA and PBS tablets were purchased from Sigma-Aldrich. When dissolved in 200 mL of water, a PBS tablet yields 10 mM phosphate buffer, 2.7 mM potassium chloride, and 137 mM sodium chloride with a pH of 7.4 at 25 $^{\circ}$ C.

2.2. Methods. **2.2.1. Monomer Synthesis.** Bis(2-methacryloyl)-oxyethyl disulfide (0.1 mmol) was mixed with 500 μ L of TCEP reducing gel (4% cross-linked beaded agarose, supplied as a 50% slurry) in one container, while each of the maleimides (\sim 0.2 mmol) was used in excess and mixed with 400–600 μ L of an appropriate organic solvent that was miscible with water (Table S1 of the Supporting Information). The separate maleimide-containing tubes were then sonicated for 5 min, and the disulfide-containing tubes were rotated for 15 min to allow the pre-reduction of the disulfide reagent. The two solutions were then mixed and rotated overnight at 22 $^{\circ}$ C while the reaction proceeded. The nine new monomers are shown in Figure 1. The reaction scheme and grafting process are presented in Figure 2. The crude mixture was then added to a spin filter and receiver tube and centrifuged at 2500 rpm for 1 min (Figure S1 of the Supporting Information). The crude product was analyzed using mass spectrometry (MS), and mass spectra are shown in Figures S2–S10 of the Supporting Information. Monomer 2 was dissolved in acetone and left uncovered in a fume hood overnight to allow the acetone to evaporate before grafting. A maleimide with just a hydrogen as an R

group was not studied because of its very high reactivity, which would unpredictably affect the grafting process.

2.2.2. High-Throughput Atmospheric-Pressure Plasma (HTP-APP). The 96-well membrane plates were presoaked in DI water overnight prior to modification. They were then filtered with 200 μ L of prefiltered DI water for 2 min with a transmembrane pressure of 68 kPa (\sim 20 in. Hg) and at room temperature. Membranes located at the base of each well in the 96-well filter plate were exposed to an APP source (model ATOMFLO, Surfx Technologies LLC, Culver City, CA) at a helium flow rate of 30.0 L min⁻¹, an oxygen flow rate of 0.4 L min⁻¹, and a source-to-membrane distance of 20 mm. The plasma source was operated at 140 V and driven by a radiofrequency power at 27.12 MHz. An XYZ Robot (Surfx Technologies LLC) was used to control the plasma source over the plate with a scan speed of 6 mm s⁻¹. Following exposure to the plasma and subsequent formation of radicals at the membrane surface, 200 μ L of the monomer solution was added to each well of the filter plate. Graft polymerization was immediately initiated at 60 \pm 1 $^{\circ}$ C for 2 h. The reaction was terminated by adding prefiltered DI water (filtered using a 0.22 μ m PES Stericup, Millipore, Billerica, MA). The 96-well membrane filter plate was then soaked and rinsed with DI water for 24 h to remove any homopolymer and unreacted monomer residue from the membrane surfaces. Finally, the plates were filtered twice with 200 μ L of prefiltered DI water for 2 min through a vacuum manifold (Pall, Port Washington, NY) using a TMP of 68 kPa (\sim 20 in. Hg). The degree of grafting was not measured because attenuated total reflection infrared spectroscopy (ATR-FTIR) does not show high absorbance peaks at this monomer concentration. This concentration is used to study the effects of surface chemistry alone, not the effects of three-dimensional chain polymerization, which requires much higher monomer concentrations (typically 1–4 M, depending upon the monomer used).

2.2.3. Static Fouling. Static fouling was conducted with 1 mg/mL BSA in PBS at room temperature for 24 h, pH 7.4, and a TMP of 68 kPa. First, 200 μ L of 1 mg/mL BSA in PBS was added to each well of the 96-well membrane plate [containing both modified and unmodified (control) membranes]. The plate was then covered and left to foul for 24 h at pH 7.4 and room temperature. After static fouling, the protein solutions were removed, and 200 μ L of pure PBS was filtered through the entire plate for 2 min at a transmembrane pressure (TMP) of 68 kPa. The permeate was collected and the UV absorbance at 977 nm read for each well. The UV absorbance at 977 nm was used with a calibration curve to determine the permeate volume. This permeate volume was used to calculate resistance (see section 2.2.5). Resistance is used to calculate the fouling index. All measurements were taken in triplicate, and error bars represent one

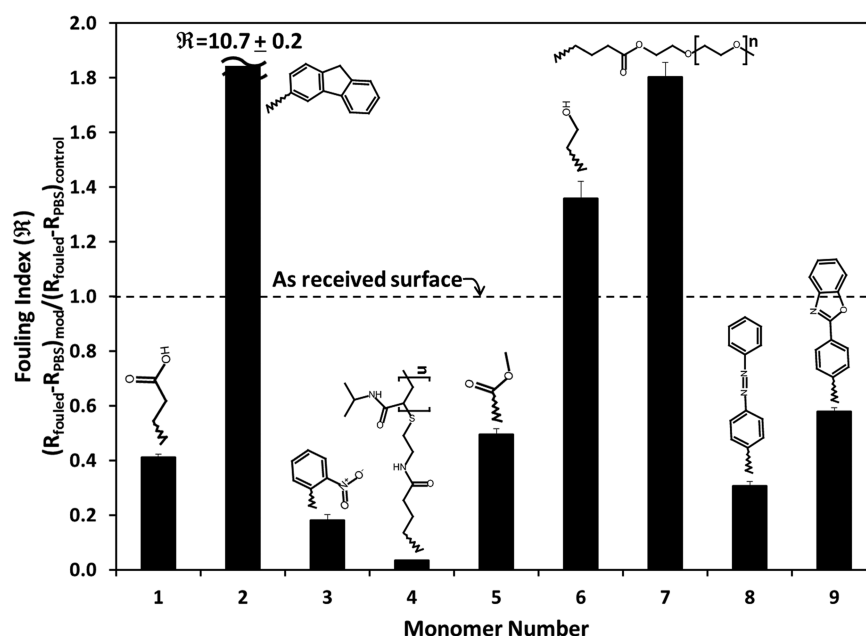


Figure 3. Fouling index values vs monomer number for all nine synthesized monomers. A chemical representation of the R groups is shown above each bar in the graph. The fouling index for monomer 2 is cut off, and its respective value is shown at the top of the bar. The performance of the as-received membrane (no modification) is shown as a dashed line at a fouling index of 1.0. The curly bond connects to the nitrogen of the maleimide ring for all of the monomers (Figure 1). All data were obtained in triplicate, and error bars represent one standard deviation.

standard deviation in Figures 3 and 5. The monomers presented in Figure S11 of the Supporting Information are shown for reference from previous work and were not tested here.

2.2.4. Dynamic Fouling. Dynamic fouling was conducted with 1 mg/mL BSA in PBS at room temperature, pH 7.4, and a TMP of 68 kPa for 2 min. First, 200 μ L of 1 mg/mL BSA in PBS was added to each well of the 96-well membrane plate [containing both modified and unmodified (control) membranes] as described in Static Fouling. The plate was then immediately filtered for 2 min at a transmembrane pressure (TMP) of 68 kPa. The permeate was collected and the UV absorbance at 280 nm read for each well. The UV absorbance at 280 nm was used with a calibration curve to determine the protein concentration. This was used with the initial protein concentration (1 mg/mL) to calculate selectivity (see section 2.2.5). All measurements were taken in triplicate, and error bars represent one standard deviation in Figure 6.

2.2.5. Assay for Protein Adhesion: High-Throughput Filtration and Evaluation. After static fouling, filtration of a PBS solution in a 96-well filter plate was performed on a multiwell plate vacuum manifold (Pall Corp., Port Washington, NY) at a constant transmembrane pressure (TMP) of 68 kPa and 22 ± 1 °C. The permeate was collected in an acrylic 96-well receiver plate (Corning Inc., Corning, NY), placed under the 96-well filter plate, establishing well-to-well alignment. The volume of permeate in each receiver well was calculated by measuring the absorbance at 977 nm of the permeate solution in the receiver plate wells using a microplate spectrophotometer (PowerWave XS, BioTek Instruments Inc., Winooski, VT) and compared with a calibration curve. Permeation flux, J_v (meters per second), is defined as $V/(At)$, where V (cubic meters) is the cumulative volume of permeate, A (square meters) is the membrane surface area, and t (seconds) is the filtration time. Membrane resistance is defined as $R = \Delta P/(\mu J_v)$, where ΔP (pascals) is TMP and μ (kilograms per meter per second) is the solution viscosity. The protein adhesion and subsequent pore blocking (i.e., antifouling performance) were measured in terms of a fouling index, \mathcal{R} :

$$\mathcal{R} = (R_{\text{Fouled}} - R_{\text{PBS}})_{\text{mod}} / (R_{\text{Fouled}} - R_{\text{PBS}})_{\text{control}} \quad (1)$$

where \mathcal{R} is defined as the ratio of the increase in resistance due to BSA fouling of the modified membrane to the control or unmodified membrane, $R_{\text{PBS,mod}}$ and $R_{\text{PBS,control}}$ are resistances to the PBS flux for

the modified and unmodified membranes before BSA fouling, respectively, and $R_{\text{Fouled,mod}}$ and $R_{\text{Fouled,control}}$ are resistances to the PBS flux for the modified and unmodified membranes after BSA fouling, respectively. An \mathcal{R} of <1 indicates that the modified membranes exhibited less BSA fouling than the control or unmodified membrane. Membrane selectivity was measured after filtration of a 1 mg/mL BSA solution in PBS for 2 min at a TMP of 68 kPa (dynamic fouling) and room temperature and is defined as

$$\psi = C_b/C_p \quad (2)$$

where C_b and C_p are the BSA concentrations in the feed (before filtration) and the permeate (after filtration), respectively. The BSA concentration in the permeate was calculated by measuring the absorbance at 280 nm of the permeate solution in the receiver plate wells and compared with a calibration curve.

2.2.6. Hansen Solubility Parameter Calculation. Hansen solubility parameters (HSPs) were calculated in an attempt to try to predict the surface properties of modified PES membrane surfaces.^{36,37} HSPs are defined as the square root of the cohesive energy density and used to characterize the physical properties of the modified surfaces. HSPs consist of three components: (i) "nonpolar" or dispersion interactions (δ_d), (ii) "polar" or permanent dipole–permanent dipole interactions (δ_p), and (iii) hydrogen bonding interactions (δ_h). Each component is estimated from the molecular physical properties of each molecular group in a monomer. Here, a group contribution method was used:

$$\delta_d = (\sum F_d)/V \quad (3)$$

$$\delta_p = (\sum F_p^2)^{1/2}/V \quad (4)$$

$$\delta_h = (\sum U_h/V)^{1/2} \quad (5)$$

where F_d ($\text{J}^{1/2} \text{cm}^{3/2} \text{mol}^{-1}$), F_p ($\text{J}^{1/2} \text{cm}^{3/2} \text{mol}^{-1}$), and U_h ($\text{J} \text{mol}^{-1}$) are the molar attraction constants for the nonpolar groups, the molar attraction constants for the polar groups, and the hydrogen bonding energy, respectively, and V ($\text{cm}^3 \text{mol}^{-1}$) is the monomer molar volume. These were tabulated using the relevant tables from a Handbook of Solubility Parameters.³⁸ Hansen solubility parameters are shown in Figure 4. They are purely theoretical and not experimental and are based on the structure of each monomer. The

results are plotted in relation to water because water interactions play a critical role during protein binding with surfaces in aqueous solutions.²¹

3. RESULTS AND DISCUSSION

3.1. Antifouling Performance of Modified PES Membranes. The filtration performance of the newly synthesized monomers, as characterized by the fouling index (\mathcal{R}), is shown in Figure 3. Monomers 1, 3–5, 8, and 9 all had \mathcal{R} values lower than those of the unmodified control membranes (<1). Monomers 1, 3, 4, and 8 performed the best (acid, zwitterionic, amide, and azo, respectively). Monomers 2, 6, and 7 performed poorer than the unmodified control membranes ($\mathcal{R} = 1.0$). Monomer 2 performed substantially worse than the others and is shown as a cutoff bar. Monomer 2 had a fouling index of 10.7 ± 0.2 . Interestingly, monomers 4 and 7 performed very differently, even though they have similar chain lengths. This could be due to the intermolecular interactions between grafted chains or the roughness of the surface. Because of the sparse grafting density used here, it was not possible to further investigate the mechanism. Using a higher graft density and comparing the surface morphology using atomic force microscopy (AFM) would be useful for further study.

We have previously reported the sessile contact angles for water drops under cyclooctane that were $62 \pm 2^\circ$ and $107 \pm 2^\circ$ for -OH (monomer 6) and -OCH₃ (monomer 7), respectively.³⁸ We can see qualitatively that the more hydrophilic the functional group, the smaller the contact angle and the lower the fouling indices (\mathcal{R} values). Thus, we surmise that water interactions play an important role in protein adhesion and hence fouling.

Next, we present an analysis of Hansen solubility parameters for different monomers and correlate their differences with protein resistance of antifouling properties.

3.2. Hansen Solubility Parameters (HSPs). Previously, we have shown that membrane fouling due to protein interactions (\mathcal{R} values) for a series of surfaces correlated with a distance parameter [i.e., distance of the modified surface locus from the water locus and from the hydrophobic control, butyl methacrylate (BMA)] from a specialized Hansen solubility plot. We attributed this to surface water interactions.²¹ The intrinsic hydration capacity of different chemical groups was calculated from tables using only the structure of a molecule. Hansen solubility parameters were then used to quantify the type of interactions that each different surface will have with a protein foulant in the presence of surrounding water molecules. Dispersion, or nonpolar (δ_d), polar (δ_p), and hydrogen bonding (δ_h) interactions were calculated using the group contribution method.^{36,37} These data are based entirely upon the structure of each monomer. They do not always predict filtration performance, so we use them as a reference to see which monomers should theoretically perform well. These parameters do not take into account the three-dimensional structure of the resultant polymer (i.e., if its functional groups are exposed or buried after graft-induced polymerization) and do not include entropic contributions. Figure 4 shows a lumped solubility parameter $(\delta_p^2 + \delta_h^2)^{1/2}$ plotted versus δ_d for the newly synthesized monomers, excluding monomers 3, 8, and 9, which could not be calculated because of insufficient database data for certain groups. BMA is included as a hydrophobic reference. The greater the distance from the water locus, the

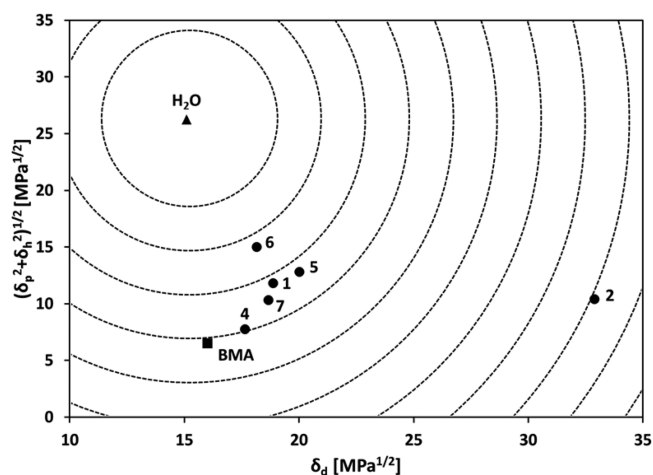


Figure 4. Hansen solubility parameters of $(\delta_p^2 + \delta_h^2)^{1/2}$ vs δ_d of synthesized monomers and water.

less affinity the monomer likely has for water. The dotted circles are used to help guide the eye.

Monomer 2 was the farthest from water and therefore should exhibit the highest fouling index. Conversely, monomers 1, 5, and 6 were the closest to the water locus and should have the lowest fouling indices. These predictions were mostly consistent with our filtration results. Monomer 6 was predicted to perform well but had a fouling index higher than that of the control membrane. This could be due to the relatively short chain length of the R group, as well as the fact that it is composed of a hydrophobic hydrocarbon chain. Monomer 7 should have performed well but performed worse, likely because of its very long chain length. This had an effect that was the opposite of that of monomer 6 because its long chain length likely blocked the pores and increased protein adhesion.

3.3. Development of Antifouling Membranes. Antifouling membranes require both a low fouling index and high permeability (low resistance to flow). In Figure 5, the fouling index is plotted against the normalized resistance, which is the ratio of resistance to flow of the modified membrane to the unmodified control membrane. Normalized resistance is a measure of additional resistance to flow imparted to the membrane from the modification of the surface alone (before fouling). A desired optimal membrane modification should exhibit properties in the direction of the arrow. Data for previously synthesized amide monomers (A1–A3, A6, and A8–A10), shown in Figure S11 of the Supporting Information, as well as three previously tested commercial monomers (PEG 9, hydroxyl 4, and BMA) are included for reference from earlier work.^{14,15,21,31,39} Membranes modified with monomers 1, 3–5, 8, and 9 all exhibited fouling indices lower than that of the control membrane (Figure 3). The best performing monomers were monomers 1, 3, and 5 because they also exhibited normalized resistances lower than that of the control membrane. All three of these monomers also had fouling indices lower than those of the best previously synthesized monomers. Monomer 6 did not perform as well as expected. It had a fouling index higher than but a resistance lower than that of the control. Both of these results can likely be attributed to the short length of the R group on this monomer. It was likely too short to have a real antifouling effect, but short enough that its effect on normalized flow resistance was negligible. Monomers 8 and 9 had resistances much higher than that of

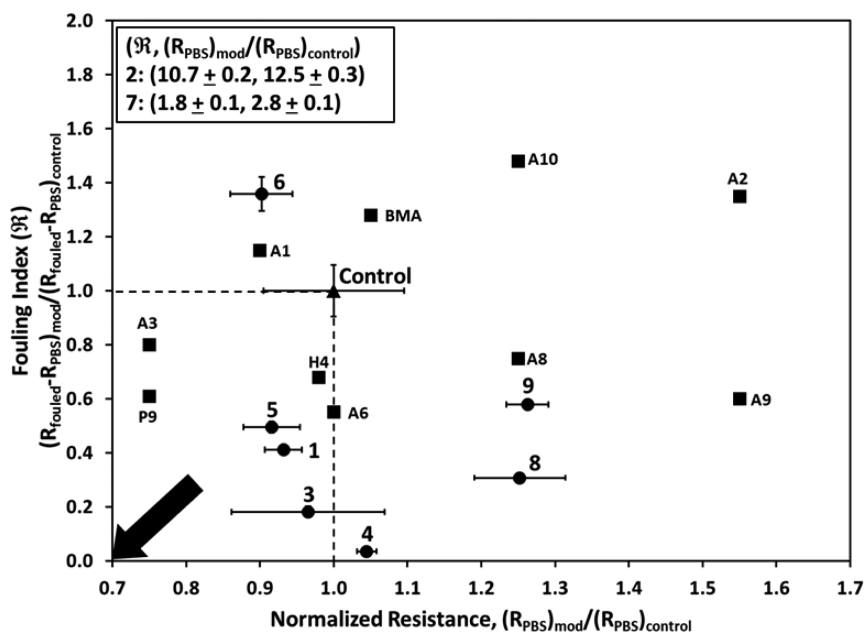


Figure 5. Performance after a static fouling test, normalized by the performance for the as-received membrane ($R_{\text{PES,control}} = 1.0 \pm 0.1$, and $R_{\text{PES,control}} = 1.0 \pm 0.1$). Several previously synthesized monomers (A1–A3, A6, and A8–A10) and some previously tested commercial monomers (PEG 9, hydroxyl 4, and BMA) are shown for reference (squares). The fouling index and normalized resistances are shown in the box at the top left for monomers 2 and 7 because they were much higher than the values of the other monomers. One standard deviation of error is shown in both the x and y directions for all newly synthesized monomers (1–9). All data were obtained in triplicate.

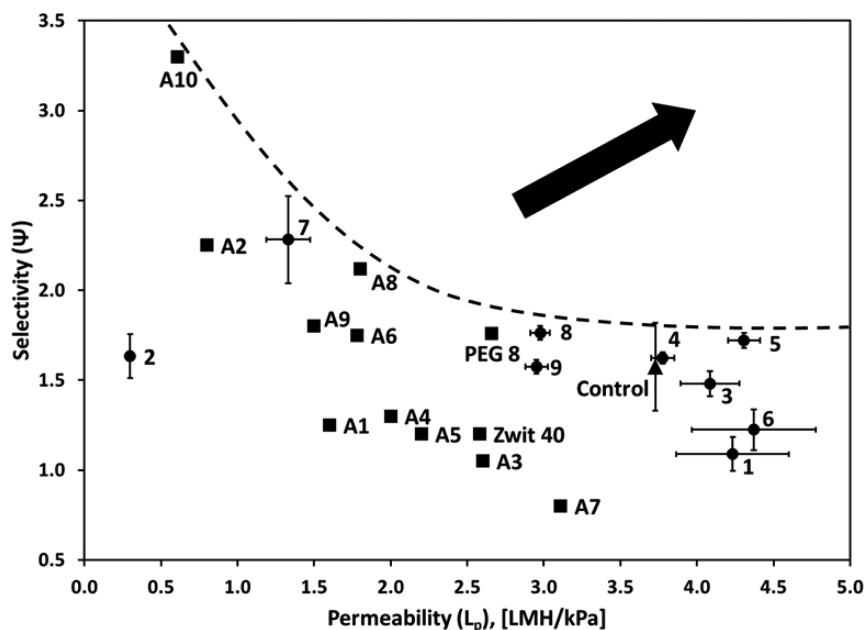


Figure 6. Performance after a dynamic fouling test. Data shown for the synthesized monomers, the as-received membrane, and the previously tested monomers (A1–A10, PEG 8, and zwitterionic 40) for reference (squares). All data were obtained in triplicate, and error bars represent one standard deviation.

the control membrane, so they are less desirable than monomers 1, 3, and 5 because they add an inherent resistance to the membrane. The worst performing monomers were monomers 2 and 7 (Figure 5, inset). Their fouling indices and normalized resistances were as follows: 10.7 ± 0.2 and 12.5 ± 0.3 for monomer 2 and 1.8 ± 0.1 and 2.8 ± 0.1 for monomer 7, respectively. Monomer 2 was very hydrophobic and therefore was expected to foul extensively, as shown. Monomer 7 was a very long PEG, which is hydrophilic, but most likely fouled because of its long chain length, as shown previously.²¹

3.4. Dynamic Fouling (Selectivity vs Permeability). In addition to antifouling properties, one also desires high selectivity and high permeability. Previously, Zydney and others^{40,41} plotted the separation factor versus permeability and found that there was an upper bound above which no current membrane separations could be achieved. Here, selectivity is plotted against permeability (Figure 6). Selectivity is measured as the ratio of the concentration of BSA in the feed to that in the permeate and is plotted against permeability. The classic trend can be seen, in that membranes with high

selectivity have low permeability and vice versa. The dashed line is drawn for reference and is not a fitted parameter.

Monomers 1, 3, 5, and 6 all exhibited permeability higher than that of the control but had selectivity similar to that of the control. Most of the previously synthesized amide monomers (squares) had permeability lower than that of the control, but some had slightly higher selectivity. Monomer 7 had the highest selectivity ($\psi = 2.3$) and low permeability ($L_p = 1.3 \pm 0.14$ LMH/kPa). Monomer 7 most likely fouled the most because of its long chain length, as shown earlier with its uncharacteristically high fouling index. Monomer 2 had the lowest permeability ($L_p = 0.3 \pm 0.02$ LMH/kPa), as predicted. The monomers with the highest permeability were monomer 6 ($L_p = 4.4 \pm 0.40$ LMH/kPa), monomer 5 ($L_p = 4.3 \pm 0.11$ LMH/kPa), and monomer 1 ($L_p = 4.2 \pm 0.37$ LMH/kPa). This is very consistent with the predictions from the Hansen solubility parameter calculations. These data support our hypothesis that water interactions play a major role in protein adhesion processes because monomers that had favorable intermolecular interactions with water performed better.

4. CONCLUSIONS

Using combinatorial chemistry that allows one to expand the breadth and depth of one's library, a set of diverse monomers were synthesized and tested employing our unique high-throughput screening platform with APP. Using membrane ultrafiltration as an example system to reduce protein adhesion (biofouling), monomers containing a carboxylic acid (monomer 1), a zwitterionic group (monomer 3), and an ester (monomer 5) performed the best from a fouling resistance viewpoint. All three of these monomers performed better than our best previously synthesized amide monomers.²¹ Our results are consistent with the fact that hydrophilic surface chemistries tend to be more protein resistant or less protein fouling. This, we suspect, is primarily due to the importance of surface–water and protein–water interactions during the protein filtration process. These interactions may also be relevant for most other biofouling events. Zwitterions have also performed well, likely because of strong intermolecular interactions required to neutralize overall charge, leading to electrostatically induced water adsorption.³² After dynamic fouling, monomers containing a carboxylic acid, zwitterionic, an ester, and a hydroxyl (monomer 6) exhibited the highest permeability. Meanwhile, the long PEG ($M_n = 2000$) (monomer 7) had the highest selectivity. Hansen solubility parameters proved to be useful for predicting which grafted polymeric surfaces would likely be antifouling. HSPs act as a guide for determining which monomers will have strong interactions with water. As stated above, this is likely critical to the protein fouling process.

■ ASSOCIATED CONTENT

Supporting Information

Solvents used, experimental schematic of the combinatorial reaction, mass spectra, and previously synthesized monomers. This material is available free of charge via the Internet at <http://pubs.acs.org>.

■ AUTHOR INFORMATION

Corresponding Author

*E-mail: belfog@rpi.edu. Telephone: (518) 276-6948.

Funding

Supported by the U.S. Department of Energy (DE-FG02-09ER16005).

Notes

The authors declare no competing financial interest.

■ ACKNOWLEDGMENTS

We thank Dr. Dmitri Zagorevski for mass spectrometry analysis, Ron Lipsky (Seahorse Labware) for discounting the 96-well filter plates, Tom Gsell and Irv Joffe (Pall Corp.) for PES membranes, Jason Nichols (GE Global, Schenectady, NY) for discussions, and Victor Schultz for his advice on maleimide solubility.

■ ABBREVIATIONS

PES, poly(ether sulfone); APP, atmospheric-pressure plasma; HTP, high-throughput; MWCO, molecular weight cutoff; BSA, bovine serum albumin; PBS, phosphate-buffered saline; TCEP, tris(2-carboxyethyl)phosphine; TMP, transmembrane pressure

■ REFERENCES

- (1) Chambers, L. D.; Stokes, K. R.; Walsh, F. C.; Wood, R. J. K. Modern Approaches to Marine Antifouling Coatings. *Surf. Coat. Technol.* **2006**, *201*, 3642–3652.
- (2) Flemming, H. C. Biofouling in Water Systems: Cases, Causes and Countermeasures. *Appl. Microbiol. Biotechnol.* **2002**, *59*, 629–640.
- (3) Townsin, R. L. The Ship Hull Fouling Penalty. *Biofouling* **2003**, *19*, 9–15.
- (4) Majumdar, P.; Lee, E.; Patel, N.; Ward, K.; Staflien, S. J.; Daniels, J.; Chisholm, B. J.; Boudjouk, P.; Callow, M. E.; Callow, J. A. Combinatorial Materials Research Applied to the Development of New Surface Coatings IX: An Investigation of Novel Antifouling/Fouling-Release Coatings Containing Quaternary Ammonium Salt Groups. *Biofouling* **2008**, *24*, 185–200.
- (5) Cassé, F.; Staflien, S. J.; Bahr, J. A.; Daniels, J.; Finlay, J. A.; Callow, J. A.; Callow, M. E. Combinatorial Materials Research Applied to the Development of New Surface Coatings V. Application of a Spinning Water-Jet for the Semi-High Throughput Assessment of the Attachment Strength of Marine Fouling Algae. *Biofouling* **2007**, *23*, 121–130.
- (6) Staflien, S.; Daniels, J.; Mayo, B.; Christianson, D.; Chisholm, B.; Ekin, A.; Webster, D.; Swain, G. Combinatorial Materials Research Applied to the Development of New Surface Coatings IV. A High-Throughput Bacterial Biofilm Retention and Retraction Assay for Screening Fouling-Release Performance of Coatings. *Biofouling* **2007**, *23*, 45–54.
- (7) Anand, G.; Zhang, F.; Linhardt, R. J.; Belfort, G. Protein-Associated Water and Secondary Structure Effect Removal of Blood Proteins from Metallic Substrates. *Langmuir* **2011**, *27*, 1830–1836.
- (8) Changani, S. D.; BelmarBeiny, M. T.; Fryer, P. J. Engineering and Chemical Factors Associated with Fouling and Cleaning in Milk Processing. *Exp. Therm. Fluid Sci.* **1997**, *14*, 392–406.
- (9) Banerjee, I.; Pangule, R. C.; Kane, R. S. Antifouling Coatings: Recent Developments in the Design of Surfaces That Prevent Fouling by Proteins, Bacteria, and Marine Organisms. *Adv. Mater.* **2011**, *23*, 690–718.
- (10) Jiang, S.; Cao, Z. Ultralow-Fouling, Functionalizable, and Hydrolyzable Zwitterionic Materials and Their Derivatives for Biological Applications. *Adv. Mater.* **2010**, *22*, 920–932.
- (11) Chang, I. S.; Le Clech, P.; Jefferson, B.; Judd, S. Membrane Fouling in Membrane Bioreactors for Wastewater Treatment. *J. Environ. Eng. (Reston, VA, U.S.)* **2002**, *128*, 1018–1029.
- (12) Le-Clech, P.; Chen, V.; Fane, T. A. G. Fouling in Membrane Bioreactors Used in Wastewater Treatment. *J. Membr. Sci.* **2006**, *284*, 17–53.

- (13) Meng, F.; Chae, S.-R.; Drews, A.; Kraume, M.; Shin, H.-S.; Yang, F. Recent Advances in Membrane Bioreactors (Mbrs): Membrane Fouling and Membrane Material. *Water Res.* **2009**, *43*, 1489–1512.
- (14) Zhou, M.; Liu, H.; Kilduff, J. E.; Langer, R.; Anderson, D. G.; Belfort, G. High Throughput Synthesis and Screening of New Protein Resistant Surfaces for Membrane Filtration. *AIChE J.* **2010**, *56*, 1932–1945.
- (15) Zhou, M.; Liu, H.; Venkiteswaran, A.; Kilduff, J.; Anderson, D. G.; Langer, R.; Belfort, G. High Throughput Discovery of New Fouling-Resistant Surfaces. *J. Mater. Chem.* **2011**, *21*, 693–704.
- (16) Holmlin, R. E.; Chen, X.; Chapman, R. G.; Takayama, S.; Whitesides, G. M. Zwitterionic Sams That Resist Nonspecific Adsorption of Protein from Aqueous Buffer. *Langmuir* **2001**, *17*, 2841–2850.
- (17) Ostuni, E.; Chapman, R. G.; Holmlin, R. E.; Takayama, S.; Whitesides, G. M. A Survey of Structure–Property Relationships of Surfaces That Resist the Adsorption of Protein. *Langmuir* **2001**, *17*, 5605–5620.
- (18) Kolb, H. C.; Finn, M.; Sharpless, K. B. Click Chemistry: Diverse Chemical Function from a Few Good Reactions. *Angew. Chem., Int. Ed.* **2001**, *40*, 2004–2021.
- (19) Velázquez, H. D.; García, Y. R.; Vandichel, M.; Madder, A.; Verpoort, F. Water-Soluble Nhc-Cu Catalysts: Applications in Click Chemistry, Bioconjugation and Mechanistic Analysis. *Org. Biomol. Chem.* **2014**, *12*, 9350–9356.
- (20) Moses, J. E.; Moorhouse, A. D. The Growing Applications of Click Chemistry. *Chem. Soc. Rev.* **2007**, *36*, 1249–1262.
- (21) Gu, M.; Vegas, A. J.; Anderson, D. G.; Langer, R. S.; Kilduff, J. E.; Belfort, G. Combinatorial Synthesis with High Throughput Discovery of Protein-Resistant Membrane Surfaces. *Biomaterials* **2013**, *34*, 6133–6138.
- (22) McNally, A.; Prier, C. K.; MacMillan, D. W. C. Discovery of an A-Amino C–H Arylation Reaction Using the Strategy of Accelerated Serendipity. *Science* **2011**, *334*, 1114–1117.
- (23) Yoon, D. Y.; Lim, E.; Kim, Y. J.; Cho, B. K.; Nam, I.-S.; Choung, J. W.; Yoo, S. A Combinatorial Chemistry Method for Fast Screening of Perovskite-Based No Oxidation Catalyst. *ACS Comb. Sci.* **2014**, *16*, 614–623.
- (24) Güell, C.; Davis, R. H. Membrane Fouling During Microfiltration of Protein Mixtures. *J. Membr. Sci.* **1996**, *119*, 269–284.
- (25) Belfort, G.; Davis, R. H.; Zydney, A. L. The Behavior of Suspensions and Macromolecular Solutions in Crossflow Microfiltration. *J. Membr. Sci.* **1994**, *96*, 1–58.
- (26) Gottschalk, U. Downstream Processing of Monoclonal Antibodies: From High Dilution to High Purity. *BioPharm Int.* **2005**, *18*, 42.
- (27) Farid, S. S. Economic Drivers and Trade-Offs in Antibody Purification Processes. *BioPharm Int.* **2009**, 38.
- (28) Pertsin, A. J.; Grunze, M. Computer Simulation of Water near the Surface of Oligo(Ethylene Glycol)-Terminated Alkanethiol Self-Assembled Monolayers. *Langmuir* **2000**, *16*, 8829–8841.
- (29) Hower, J. C.; He, Y.; Bernards, M. T.; Jiang, S. Understanding the Nonfouling Mechanism of Surfaces through Molecular Simulations of Sugar-Based Self-Assembled Monolayers. *J. Chem. Phys.* **2006**, *125*, 214704.
- (30) Nomura, K.; Nakaji-Hirabayashi, T.; Gemmei-Ide, M.; Kitano, H.; Noguchi, H.; Uosaki, K. Sum-Frequency Generation Analyses of the Structure of Water at Amphoteric Sam-Liquid Water Interfaces. *Colloids Surf., B* **2014**, *121*, 264–269.
- (31) Jeon, S. I.; Lee, J. H.; Andrade, J. D.; De Gennes, P. G. Protein–Surface Interactions in the Presence of Polyethylene Oxide: I. Simplified Theory. *J. Colloid Interface Sci.* **1991**, *142*, 149–158.
- (32) Chen, S.; Zheng, J.; Li, L.; Jiang, S. Strong Resistance of Phosphorylcholine Self-Assembled Monolayers to Protein Adsorption: Insights into Nonfouling Properties of Zwitterionic Materials. *J. Am. Chem. Soc.* **2005**, *127*, 14473–14478.
- (33) Li, G.; Cheng, G.; Xue, H.; Chen, S.; Zhang, F.; Jiang, S. Ultra Low Fouling Zwitterionic Polymers with a Biomimetic Adhesive Group. *Biomaterials* **2008**, *29*, 4592–4597.
- (34) Murthy, R.; Shell, C. E.; Grunlan, M. A. The Influence of Poly(Ethylene Oxide) Grafting Via Siloxane Tethers on Protein Adsorption. *Biomaterials* **2009**, *30*, 2433–2439.
- (35) Jeon, S. I.; Andrade, J. D. Protein–Surface Interactions in the Presence of Polyethylene Oxide: II. Effect of Protein Size. *J. Colloid Interface Sci.* **1991**, *142*, 159–166.
- (36) Barton, A. F. M. *Handbook of Solubility Parameters and Other Cohesion Parameters*, 2nd ed.; CRC Press: Boca Raton, FL, 1991.
- (37) Hansen, C. M. *Hansen Solubility Parameters: A User's Handbook*, 2nd ed.; Taylor & Francis Group, LLC: Boca Raton, FL, 2007.
- (38) Sethuraman, A.; Han, M.; Kane, R. S.; Belfort, G. Effect of Surface Wettability on the Adhesion of Proteins. *Langmuir* **2004**, *20*, 7779–7788.
- (39) Gu, M.; Kilduff, J. E.; Belfort, G. High Throughput Atmospheric Pressure Plasma-Induced Graft Polymerization for Identifying Protein-Resistant Surfaces. *Biomaterials* **2012**, *33*, 1261–1270.
- (40) Mehta, A.; Zydney, A. L. Permeability and Selectivity Analysis for Ultrafiltration Membranes. *J. Membr. Sci.* **2005**, *249*, 245–249.
- (41) Robeson, L. M. Correlation of Separation Factor Versus Permeability for Polymeric Membranes. *J. Membr. Sci.* **1991**, *62*, 165–185.